Computational Particle Mechanics manuscript No.
(will be inserted by the editor)

On the convergence of the Generalized Finite Difference Method for solving a chemotaxis system with no chemical diffusion

J.J. Benito · A. García · L. Gavete · M. Negreanu · F. Ureña · A.M. Vargas

Received: date / Accepted: date

Abstract This paper focuses on the numerical analysis of a discrete version of a nonlinear reaction-diffusion system consisting of an ordinary equation coupled to a quasilinear parabolic PDE with a chemotactic term. The parabolic equation of the system describes the behavior of a biological species, while the ordinary equation defines the concentration of a chemical substance. The system also includes a logistic-like source, which limits the growth of the biological species and presents a time-periodic asymptotic behavior. We study the convergence of the explicit discrete scheme obtained by means of the Generalized Finite Difference method and prove that the non-negative numerical solutions in two dimensional space preserve the asymptotic behavior of the continuous ones. Using different functions and long-time simulations, we illustrate the efficiency of the developed numerical algorithms in the sense of the convergence in space and in time.

Keywords Chemotaxis systems · Generalized Finite Difference · Meshless method · Asymptotic stability.

J.J. Benito
UNED, ETSII, Madrid, Spain.

A. García
UNED, ETSII, Madrid, Spain.

L. Gavete
UPM, ETSIM, Madrid, Spain.

M. Negreanu
Instituto de Matemática Interdisciplinar, Depto. de Análisis Matemático y Matemática Aplicada, Universidad Complutense de Madrid, 28040 Madrid, Spain.

F. Ureña
UNED, ETSII, Madrid, Spain.

A.M. Vargas
Universidad Complutense de Madrid, 28040 Madrid, Spain. E-mail: antonvar@ucm.es

1 Introduction

In this paper we use a meshless method called Generalized Finite Difference Method (GFDM) to study the discretization of the nonlinear system of differential equations

$$\begin{cases} \dfrac{\partial U}{\partial t} = \Delta U - div(\chi U \nabla V) + \mu U(1 + f(\mathbf{x}, t) - U), & \mathbf{x} \in \Omega, \quad t > 0, \\ \dfrac{\partial V}{\partial t} = h(U, V), & \mathbf{x} \in \Omega, \quad t > 0, \\ U(\mathbf{x}, 0) = U_0(\mathbf{x}), V(\mathbf{x}, 0) = V_0(\mathbf{x}), & \mathbf{x} \in \Omega, \\ \dfrac{\partial U}{\partial n} = \dfrac{\partial V}{\partial n} = 0, & \mathbf{x} \in \partial\Omega, \quad t > 0 \end{cases} \tag{1}$$

in a smooth bounded domain $\Omega \subset \mathbb{R}^2$ with positive constant chemotaxis χ and $\mu > 0$. The logistic-like source limits the growth of the biological species and it presents a time-periodic asymptotic behavior in the sense: f is a bounded given function fulfilling

$$\|f(\mathbf{x}, t) - f^*(t)\|_{L^\infty(\Omega)} \to 0, \quad \text{as} \quad t \to \infty,$$

with $f^*(t)$ being a time-periodic function independent of the space variable "$\mathbf{x}$". The parabolic equation describes the behavior of a biological species "U" and the ordinary differential equation patterns the concentration of a chemical substance "V". The regular function h increases as "U" increases and states the production of the chemical species. In the recently published article [16], the authors prove that for all sufficiently smooth initial data $U(\mathbf{x}, 0) = U_0(\mathbf{x})$, $V(\mathbf{x}, 0) = V_0(\mathbf{x})$, $\mathbf{x} \in \Omega$, the problem possesses a unique global-in-time classical solution that is bounded in $\Omega \times (0, \infty)$, with $\Omega \subset \mathbb{R}^n$, for $n \geq 1$. We prove that the convergence in space and in time of the classical solution is maintained for the discrete model.

The system arises in chemotaxis, the phenomenon whereby living organisms respond to a chemical substance by motion and rearrangement (taxis). If they move toward the higher concentration of the chemical substance one is referring to *positive taxis* and otherwise, away from it, to *negative taxis*, i.e., they may aggregate, or they may disperse.

Mathematical models for chemotaxis have been studied since 1970s when Keller and Segel proposed a model that leads to aggregation of certain types of bacteria [8]–[9]. The first model involved the density distribution of the bacteria and the chemical concentration in a coupled system of partial differential equation. Since then, other models have been proposed and studied in order to understand the mechanism that causes the aggregation of myxobacteria; for instance, Othmer and Stevens in [17] derived the following system of partial differential equations

$$\begin{cases} \dfrac{\partial U}{\partial t} = div(\nabla U - U\chi(V)\nabla V), & \mathbf{x} \in \Omega, \quad t > 0, \\ \dfrac{\partial V}{\partial t} = h(U, V), & \mathbf{x} \in \Omega, \quad t > 0, \end{cases} \tag{2}$$

where $\chi(V)$ is the chemotactic sensitivity of the bacteria. Functions $\chi(V)$ and $h(U,V)$ depend on the nature of the interaction between the bacteria and the chemical stimulus.
Chemotaxis is an important process in many medical and biological applications including bacteria/cell aggregation, pattern formation mechanisms, the movement of human blood neutrophils and tumor growth. The tumor secretes chemical species that attract the nearby endothelial cells, which form the surface of capillary blood vessels. In this way new blood vessels sprout towards the tumor and begin to provide it with additional nourishment. The phenomenon of sprouting of new blood vessels is called angiogenesis. The models could involve several diffusing populations and several chemical species. Many models of angiogenesis with one diffusing population and two nondiffusing ones were studied by Anderson and Chaplain in [1].
There are several examples in the nature of species with periodic behavior, for instance, in the movement of the amebas *Dictyostelium discoideum* towards its center of aggregation, the medium velocity is periodic (see Steinbock, Hashimoto and Müller [18]), in Dunn and Zicha [6] it is observed periodicity in the chemotaxis of the human neutrophils and also it is referred in Zusman, Scott, Yang and Kirby [21] in the movement of the *Myxococcus xanthus*.
In a mathematical view, global existence and behavior of solutions are fundamental theme. However, problem (1) has some difficult points caused by the logistic term and by generalization of function h. To overcome the difficulty, Negreanu, Tello and Vargas [12,13], [16] (see also the references therein) built a technical way to prove global existence and asymptotic behavior of solutions of (1).
Throughout the article we use the notation $\Omega_t = \Omega \times (0,t)$, for $t \in (0,\infty]$ and we work under the following hypotheses (see [16] for more details):

1. Function h fulfills
$$h \in W^{1,\infty}_{loc}(\mathbb{R}_+ \times \mathbb{R}) \cap C^2(\mathbb{R}^2_+); \tag{3}$$
$$\frac{\partial h}{\partial U} > 0, \quad \frac{\partial h}{\partial V} < 0, \quad 0 \le h(0,0) < \mu\varepsilon/(2\chi), \tag{4}$$
for some positive $\varepsilon > 0$ and
$$-h(0,V) \le ce^{\chi V}, \quad \frac{\partial h}{\partial V} + U\chi\frac{\partial h}{\partial U} \le -\epsilon_v/2, \text{ with } \epsilon_v, c > 0. \tag{5}$$
2. For a given constant $\mathcal{C} := \mathcal{C}(u_0, \|f\|_{L^\infty(\Omega)}, \mu, \chi, c\}$ (see Lemma 2 in [16]), for some positive $\epsilon_0 > 0$, h fulfills
$$\limsup_{s\to\infty} h\left(\mathcal{C}e^{\chi s}, s\right) \le -\epsilon_0. \tag{6}$$
3. There exists a periodic function f^* verifying
$$\|f(x,t) - f^*(t)\|_{L^\infty(\Omega)} \to 0, \quad \text{as} \quad t \to \infty, \tag{7}$$
$$\inf_{x\in\Omega} f(x,t) < f^*(t) < \sup_{x\in\Omega} f(x,t) \tag{8}$$

and for ε as in (4), function f checks

$$-1+\varepsilon < f(x,t). \tag{9}$$

The above conditions cover the examples $h(U,V) = Ue^{-\chi V} - aV$, with $a > 0$ and $h(U,V) = (Ue^{-\chi V} + V)/(1+V) - V$ which we use in our numerical study. We denote by U^* and V^* the solutions of the ODE's equations

$$U_t^* = \mu U^*(1 - U^* + f^*), \quad U^*(0) = U_0^*, \tag{10}$$

$$V_t^* = h(U^*, V^*), \quad V^*(0) = V_0^*. \tag{11}$$

In order to obtain the asymptotic properties of the solutions of (1), we introduce (as in [15], [16]) the explicit expression of U^*

$$U^*(t) = \frac{U_0^* e^{\int_0^t \mu(1+f^*(s))ds}}{1 + U_0^* \displaystyle\int_0^t \mu e^{\int_0^\tau \mu(1+f^*(s))ds} d\tau}, \tag{12}$$

for U_0^* defined by

$$U_0^* := \frac{e^{\int_0^T \mu(1+f^*(s))ds} - 1}{\mu \int_0^T e^{\int_0^\tau \mu(1+f^*(s))ds} d\tau}$$

and f^* as in (7). Notice that U^* satisfies equation (10) and it is homogeneous in space and periodic in time function, [14]. In [16], the global existence and uniqueness of the bounded solution (U,V) of (1) is done for any nonnegative initial data $(U_0, V_0) \in (L^\infty(\Omega) \cap W^{1,s}(\Omega))^2$. Moreover, they proved that

$$\|U(\mathbf{x},t) - U^*(t)\|_{L^2(\Omega)} \to 0 \quad \|V(\mathbf{x},t) - V^*(t)\|_{L^2(\Omega)} \to 0, \; as \; t \to \infty.$$

In this paper we obtain the conditional convergence of the GDF scheme for the discretization of (1) and we give the explicit conditions that the time increment, Δt must fulfil in order to have it. The discrete numerical solution converges to the asymptotic periodic functions $U^*(t)$, $V^*(t)$). This means that some environmental periodicity conditions affect the behavior of the populations' density of a biological species, "U" and a chemical substance, "V", related by a chemotactic process. We also illustrate with our experiments that the Generalized Finite Difference Method solves this strongly coupled highly nonlinear parabolic-ODE system efficiently and with high accuracy over regular and irregular domains. In other words, we prove that the discrete solution obtained by applying GFD method to (1) preserves the same behavior of the continuous one.

The GDF method was first derived by Jensen [7] and Liszka and Orkisz [10]. Benito, Gavete and Ureña [2,3,19] have studied the influence of several factors and developed the explicit formulae and h-adaptive method for the solution of the PDEs in 2D. The implementation of the GFDM for the Keller-Segel chemotaxis model with parabolic-elliptic coupling was recently done in [20] where the authors proved the convergence of the explicit method and gave the

conditions of convergence. Recently, numerical solutions of chemotaxis systems are being investigated. For instance, MacDonald *et al.* used a moving mesh finite element method [11]. In [5] Dehghan *et al.* used radial basis collocation method for solving similar systems.
The paper is organized as follows: in Section 2 we introduce some explicit formulae using the Generalized Finite Difference method. We study the convergence of the GFD explicit scheme and we prove the main result of the paper, Theorem 1. In Section 3, extensive numerical experiments (convergence studies in space and in time, long-time simulations, etc.) are presented to illustrate the efficiency and robustness of the developed numerical algorithms. We finally present some conclusions.

2 GFDM explicit scheme

Consider a domain $\Omega \subset \mathbb{R}^2$ and let $M = \{\mathbf{x}_1, \dots, \mathbf{x}_N\} \subset \Omega$ be a discretization of it with N points. For each $\mathbf{x}_0 \in M$, we define $E_s = \{\mathbf{x}_0; \mathbf{x}_1, \dots, \mathbf{x}_s\} \subset M$, where $\mathbf{x}_i$ $(i = 1, \dots, s)$ can be chosen in several ways, by different criteria.
We call $\mathbf{x}_i = (x_i, y_i)$ and we denote by $h_i := x_i - x_0$ and $k_i := y_i - y_0$. Let be $F \in \mathcal{C}^4(\Omega)$. Since no confusion with the initial data of F is possible, we write in this section $F_0 = F(\mathbf{x}_0) = F(x_0, y_0)$ and $F_i = F(\mathbf{x}_i)$. By Taylor series expansion, for $i = 1, ..., s$, we have :

$$F_i = F_0 + h_i \frac{\partial F_0}{\partial x} + k_i \frac{\partial F_0}{\partial y} + \frac{1}{2}\left(h_i^2 \frac{\partial^2 F_0}{\partial x^2} + k_i^2 \frac{\partial^2 F_0}{\partial y^2} + 2h_i k_i \frac{\partial^2 F_0}{\partial x \partial y} \right) + ... \quad (13)$$

By ignoring the third and higher order terms in (13), we obtain a second order approximation f_i of F in $\mathbf{x}_i$. Moreover, we take the vector

$$\boldsymbol{D}_5 = \left\{ \frac{\partial f_0}{\partial x}, \frac{\partial f_0}{\partial y}, \frac{\partial^2 f_0}{\partial x^2}, \frac{\partial^2 f_0}{\partial y^2}, \frac{\partial^2 f_0}{\partial x \partial y} \right\}. \quad (14)$$

In this way, we can obtain an approximation of function F_i in terms of the coefficients of $\mathbf{D}_5$. In order to determine these, we minimize with respect to the partial derivatives the following function

$$\begin{aligned} B(f) = \sum_{i=1}^{s} [(f_0 - f_i) + h_i \frac{\partial f_0}{\partial x} + k_i \frac{\partial f_0}{\partial y} + \\ + \frac{1}{2}(h_i^2 \frac{\partial^2 f_0}{\partial x^2} + k_i^2 \frac{\partial^2 f_0}{\partial y^2} + 2h_i k_i \frac{\partial^2 f_0}{\partial x \partial y})]^2 w_i^2 \end{aligned} \quad (15)$$

where $w_i = w(h_i, k_i)$ are positive symmetrical monotone decreasing weighting functions. One arrives then to the following system of linear equations

$$\boldsymbol{A}(h_i, k_i, w_i)\boldsymbol{D}_5^T = \boldsymbol{b}(h_i, k_i, w_i, u_0, u_i), \quad (16)$$

where

$$\boldsymbol{A} = \begin{pmatrix} h_1 & h_2 & \cdots & h_s \\ k_1 & k_2 & \cdots & k_s \\ \vdots & \vdots & \vdots & \vdots \\ h_1k_1 & h_2k_2 & \cdots & h_sk_s \end{pmatrix} \begin{pmatrix} \omega_1^2 & & & \\ & \omega_2^2 & & \\ & & \cdots & \\ & & & \omega_s^2 \end{pmatrix} \begin{pmatrix} h_1 & k_1 & \cdots & h_1k_1 \\ h_2 & k_2 & \cdots & h_2k_2 \\ \vdots & \vdots & \vdots & \vdots \\ h_s & k_s & \cdots & h_sk_s \end{pmatrix}.$$

Some assumptions on the selection criteria of the nodes of E_s must be made in order to guarantee that $\mathbf{A}$ is positive definite (see [20] for more details on the selection criteria and the weighting functions). By solving system (16), we can find the discretization of the spatial derivatives as functions of f_0 and f_i:

$$\begin{cases} \dfrac{\partial f(\mathbf{x}_0, n\Delta t)}{\partial x} = -m_{01} f_0^n + \displaystyle\sum_{i=1}^{s} m_{i1} f_i^n + \mathcal{O}(h_i^2, k_i^2),\ with\, m_{01} = \sum_{i=1}^{s} m_{i1}, \\ \dfrac{\partial f(\mathbf{x}_0, n\Delta t)}{\partial y} = -m_{02} f_0^n + \displaystyle\sum_{i=1}^{s} m_{i2} f_i^n + \mathcal{O}(h_i^2, k_i^2),\ with\, m_{02} = \sum_{i=1}^{s} m_{i2}, \\ \dfrac{\partial^2 f(\mathbf{x}_0, n\Delta t)}{\partial x^2} = -m_{03} f_0^n + \displaystyle\sum_{i=1}^{s} m_{i3} f_i^n + \mathcal{O}(h_i^2, k_i^2),\ with\, m_{03} = \sum_{i=1}^{s} m_{i3}, \\ \dfrac{\partial^2 f(\mathbf{x}_0, n\Delta t)}{\partial y^2} = -m_{04} f_0^n + \displaystyle\sum_{i=1}^{s} m_{i4} f_i^n + \mathcal{O}(h_i^2, k_i^2),\ with\, m_{04} = \sum_{i=1}^{s} m_{i4}, \\ \dfrac{\partial^2 f(\mathbf{x}_0, n\Delta t)}{\partial x \partial y} = -m_{05} f_0^n + \displaystyle\sum_{i=1}^{s} m_{i5} f_i^n + \mathcal{O}(h_i^2, k_i^2),\ with\, m_{05} = \sum_{i=1}^{s} m_{i5}. \end{cases} \tag{17}$$

Remark 21 *For simplicity, for the discretization of the laplacian operator, we write*

$$\Delta f(\boldsymbol{x}_0, n\Delta t) = -m_{00} f_0^n + \sum_{i=1}^{s} m_{i0} f_i^n,$$

where $m_{00} = m_{03} + m_{04}$ *and* $m_{i0} = m_{i3} + m_{i4}$.

The time derivative is approximated by

$$\frac{\partial f(x_0, y_0, n\Delta t)}{\partial t} = \frac{f_0^{n+1} - f_0^n}{\Delta t} + \mathcal{O}(\Delta t). \tag{18}$$

Hence, we obtain the following 2-dimensional GFD explicit scheme:

$$\begin{cases} u_0^{n+1} = u_0^n + \Delta t \left[-m_{00} u_0^n + \displaystyle\sum_{i=1}^{s} m_{i0} u_i^n - \chi u_0^n \left(-m_{00} v_0^n + \sum_{i=1}^{s} m_{i0} v_i^n \right) \right] \\ \qquad - \chi \Delta t \left(-m_{01} u_0^n + \displaystyle\sum_{i=1}^{s} + m_{i1} u_i^n \right) \left(-m_{01} v_0^n + \sum_{i=1}^{s} m_{i1} v_i^n \right) \\ \qquad - \chi \Delta t \left(-m_{02} u_0^n + \displaystyle\sum_{i=1}^{s} + m_{i2} u_i^n \right) \left(-m_{02} v_0^n + \sum_{i=1}^{s} m_{i2} v_i^n \right) \\ \qquad + \Delta t \mu u_0^n \left[1 - u_0^n + f(\mathbf{x}_0, n\Delta t) \right] \\ v_0^{n+1} = v_0^n + h(u_0^n, v_0^n) \Delta t. \end{cases} \tag{19}$$

The main result regarding the convergence of the proposed numerical scheme (19) is as follows:

Theorem 1 *Let U, V be the exact solution of (1). Let be $\frac{\partial h}{\partial V}(U,V) < 0$, then the GFDM explicit scheme (19) is convergent if*

$$\frac{1}{\alpha - \frac{\partial h}{\partial V}} < \Delta t < \frac{3}{\alpha - \frac{\partial h}{\partial V}} \tag{20}$$

where

$$\begin{aligned}
\alpha := \Bigg| & -m_{00}(1+\chi V_0^n) - \chi[(m_{01})^2 + (m_{02})^2]v_0^n \\
& + \chi m_{01} \sum_{i=1}^{s} m_{i1} v_0^n + \chi m_{02} \sum_{i=1}^{s} m_{i2} v_0^n - \chi \sum_{i=1}^{s} m_{i0} v_i^n \\
& + \mu[1 - (u_0^n + U_0^n) + f(\boldsymbol{x}_0, n\Delta t)]\Bigg| + \Delta t \Bigg(\sum_{i=1}^{s} |m_{i0}| \\
& + \chi |m_{01}| V_0^n \sum_{i=1}^{s} |m_{i1}| + \chi \left| \sum_{i=1}^{s} m_{i1} v_i^n \right| \sum_{i=1}^{s} |m_{i1}| \\
& + \chi \left| \sum_{i=1}^{s} m_{i2} v_i^n \right| \sum_{i=1}^{s} |m_{i2}| + \chi |m_{02}| V_0^n \sum_{i=1}^{s} |m_{i2}| \Bigg).
\end{aligned} \tag{21}$$

Proof Let u_j^n be the approximated u–solution at time $n\Delta t$ (similarly v_j^n) and U_j^n the value of the exact $U-$ solution (similarly V_j^n). Also, we call $\tilde{u}_j^n = u_j^n - U_j^n$ and $\tilde{v}_j^n = v_j^n - V_j^n$. Let us take the difference between the GFD scheme (19) and the expression for the exact solution. We obtain the following:

$$
\begin{aligned}
\tilde{u}_0^{n+1} = \tilde{u}_0^n + \Delta t \Bigg[& - m_{00}\tilde{u}_0^n + \sum_{i=1}^{s} m_{i0}\tilde{u}_i^n - \chi[(m_{01})^2 + \\
& + (m_{02}^2)][\tilde{u}_0^n v_0^n - U_0^n \tilde{v}_0^n] + \chi m_{01}\tilde{u}_0^n \sum_{i=1}^{s} m_{i1} v_i^n + \\
& + \chi m_{01} U_0^n \sum_{i=1}^{s} m_{i1}\tilde{v}_i^n + \chi m_{01}\tilde{v}_0^n \sum_{i=1}^{s} m_{i1} u_i^n \\
& + \chi m_{01} V_0^n \sum_{i=1}^{s} m_{i1}\tilde{u}_i^n - \left(\sum_{i=1}^{s} m_{i1}\tilde{u}_i^n\right)\left(\sum_{i=1}^{s} m_{i1} v_i^n\right) \\
& - \left(\sum_{i=1}^{s} m_{i1} U_i^n\right)\left(\sum_{i=1}^{s} m_{i1}\tilde{v}_i^n\right) + \chi m_{02}\tilde{u}_0^n \sum_{i=1}^{s} m_{i2} v_i^n \\
& + \chi m_{02} U_0^n \sum_{i=1}^{s} m_{i2}\tilde{v}_i^n + \chi m_{02}\tilde{v}_0^n \sum_{i=1}^{s} m_{i2} u_i^n + \chi m_{02} V_0^n \sum_{i=1}^{s} m_{i2}\tilde{u}_i^n \\
& - \left(\sum_{i=1}^{s} m_{i2}\tilde{u}_i^n\right)\left(\sum_{i=1}^{s} m_{i2} v_i^n\right) - \left(\sum_{i=1}^{s} m_{i2} U_i^n\right)\left(\sum_{i=1}^{s} m_{i2}\tilde{v}_i^n\right) \\
& + \mu\tilde{u}_0^n [1 - (u_0^n + U_0^n) + f(\mathbf{x}_0, n\Delta t)] \Bigg].
\end{aligned}
\tag{22}
$$

After rearranging the terms, it yields:

$$
\begin{aligned}
\tilde{u}_0^{n+1} = \tilde{u}_0^n \Bigg[1 - \Delta t \Bigg(& -m_{00}(1+\chi V_0^n) - \chi[(m_{01})^2 + (m_{02})^2] v_0^n \\
& + \chi m_{01} \sum_{i=1}^{s} m_{i1} v_0^n + \chi m_{02} \sum_{i=1}^{s} m_{i2} v_0^n - \chi \sum_{i=1}^{s} m_{i0} v_i^n \\
& + \mu[1 - (u_0^n + U_0^n) + f(\mathbf{x}_0, n\Delta t)] \Bigg) \Bigg] + \\
& + \tilde{v}_0^n \chi \Delta t \Bigg[-[(m_{01})^2 + (m_{02})^2] U_0^n + m_{01} \sum_{i=1}^{s} m_{i1} u_i^n + \\
& + m_{02} \sum_{i=1}^{s} m_{i2} u_i^n + m_{00} u_0^n \Bigg] + \Delta t \Bigg[\sum_{i=1}^{s} m_{i0} \tilde{u}_i^n + \\
& + \chi m_{01} V_0^n \sum_{i=1}^{s} m_{i1} \tilde{u}_i^n - \chi \left(\sum_{i=1}^{s} m_{i1} \tilde{u}_i^n \right) \left(\sum_{i=1}^{s} m_{i1} v_i^n \right) \\
& - \chi \left(\sum_{i=1}^{s} m_{i2} \tilde{u}_i^n \right) \left(\sum_{i=1}^{s} m_{i2} v_i^n \right) + \chi m_{02} V_0^n \sum_{i=1}^{s} m_{i2} \tilde{u}_i^n \Bigg] \\
& + \chi \Delta t \Bigg[m_{01} U_i^n \sum_{i=1}^{s} m_{i1} \tilde{v}_i^n - \left(\sum_{i=1}^{s} m_{i1} U_i^n \right) \left(\sum_{i=1}^{s} m_{i1} \tilde{v}_i^n \right) \\
& - \left(\sum_{i=1}^{s} m_{i2} U_i^n \right) \left(\sum_{i=1}^{s} m_{i2} \tilde{v}_i^n \right) + m_{02} U_i^n \sum_{i=1}^{s} m_{i2} \tilde{v}_i^n \Bigg].
\end{aligned} \tag{23}
$$

We now take bounds and call $\tilde{u}^n = \max_{i=0,\dots,s}\{|\tilde{u}_i^n|\}$ (the same applies for $\tilde{v}^n$). Then, we get

$$\begin{aligned}
\tilde{u}^{n+1} \leq \tilde{u}^n \Bigg[\Bigg| 1 - \Delta t \Bigg(& -m_{00}(1+\chi V_0^n) - \chi[(m_{01})^2 + (m_{02})^2]v_0^n \\
& + \chi m_{01}\sum_{i=1}^{s} m_{i1}v_0^n + \chi m_{02}\sum_{i=1}^{s} m_{i2}v_0^n - \chi\sum_{i=1}^{s} m_{i0}v_i^n \\
& + \mu[1-(u_0^n+U_0^n) + f(\mathbf{x}_0, n\Delta t)]\Bigg)\Bigg| + \Delta t\Bigg(\sum_{i=1}^{s}|m_{i0}| \\
& + \chi|m_{01}|V_0^n\sum_{i=1}^{s}|m_{i1}| + \chi\left|\sum_{i=1}^{s} m_{i1}v_i^n\right|\sum_{i=1}^{s}|m_{i1}| \\
& + \chi\left|\sum_{i=1}^{s} m_{i2}v_i^n\right|\sum_{i=1}^{s}|m_{i2}| + \chi|m_{02}|V_0^n\sum_{i=1}^{s}|m_{i2}|\Bigg)\Bigg] + \\
& + \tilde{v}^n\chi\Delta t\Bigg[\Bigg| -[(m_{01})^2 + (m_{02})^2]U_0^n + m_{01}\sum_{i=1}^{s} m_{i1}u_i^n \\
& + m_{02}\sum_{i=1}^{s} m_{i2}u_i^n + m_{00}u_0^n\Bigg| + |m_{01}|U_i^n\sum_{i=1}^{s}|m_{i1}| \\
& + \left|\sum_{i=1}^{s} m_{i1}U_i^n\right|\sum_{i=1}^{s}|m_{i1}| + \left|\sum_{i=1}^{s} m_{i2}U_i^n\right|\sum_{i=1}^{s}|m_{i2}| \\
& + |m_{02}|U_i^n\sum_{i=1}^{s}|m_{i2}|\Bigg].
\end{aligned} \tag{24}$$

For the second equation of (1) we have

$$\tilde{v}_0^{n+1} = \tilde{v}_0^n + \Delta t \frac{\partial h}{\partial U}\bigg|_{(\xi, v_0^n)} \tilde{u}_0^n + \Delta t \frac{\partial h}{\partial V}\bigg|_{(u_0^n, \eta)} \tilde{v}_0^n, \tag{25}$$

where we have applied the Mean Value Theorem twice for some $\xi \in (u_0^n, U_0^n) \cap (U_0^n, u_0^n)$, $\eta \in (v_0^n, V_0^n) \cap (V_0^n, v_0^n)$. Hence, by taking again the maximum for all indices $i = 0, ..., s$, we reach the expression

$$\tilde{v}^{n+1} \leq \tilde{u}^n \left|\frac{\partial h}{\partial U}\right| + \tilde{v}^n \left|1 + \Delta t \frac{\partial h}{\partial V}\right|. \tag{26}$$

We rewrite the last expression in matrix form, in the following sense

$$\begin{pmatrix} \tilde{u}^{n+1} \\ \tilde{v}^{n+1} \end{pmatrix} \leq \begin{pmatrix} |1 - \Delta t \cdot \alpha| & B \\ C & |1 + \Delta t \partial_V h| \end{pmatrix} \begin{pmatrix} \tilde{u}^n \\ \tilde{v}^n \end{pmatrix}. \tag{27}$$

The characteristic polynomial of the square matrix has, at most, two roots fulfilling

$$\Big| |1 - \Delta t \cdot \alpha| + |1 + \Delta t \partial_V h| \Big| \leq |\lambda_1 + \lambda_2| \leq |\lambda_1| + |\lambda_2| < 1. \tag{28}$$

If we impose

$$\left| 2 - \Delta t \left(\alpha - \frac{\partial h}{\partial V} \right) \right| < 1, \tag{29}$$

then (28) is verified. Therefore, the LHS inequality leads us to

$$\Delta t < \frac{3}{\alpha - \frac{\partial h}{\partial V}}, \tag{30}$$

whereas the second one

$$\Delta t > \frac{1}{\alpha - \frac{\partial h}{\partial V}}. \tag{31}$$

Notice that the denominator in (30)–(31) is positive due to assumption (4), i.e., $\partial_V h < 0$. So Δt can be always chosen such that the GFD explicit scheme (19) is convergent.

$\square$

Remark 22 *Observe that (4) is enough to guarantee the convergence without adding extra assumptions on the problem.*

3 Numerical examples

In this section we show the numerical results obtained by solving the system (1), using two irregular clouds of points as seen in Figure 1 (441 nodes in each one) in the domain $\Omega = [0,1] \times [0,1]$. We use an 8-node scheme, chosen by the distance criterion together with weight function $w = \frac{1}{dist^4}$. For all numerical examples we put $\Delta t = 0.001$.

Remark 31 *Note that in the following examples we compare the numerical solution of the problem with the asymptotic solution (not the exact one, since there is no explicit known solution). This explains the possible difference between our numerical values and the continuous ones at small times. Also notice that we may choose a very distant initial data (computed in l^∞ norm) from the asymptotic limit, provided enough regularity, and this may result in a difference between the discrete and continuous values at small times. The aim of this paper is to obtain the numerical validation of asymptotic convergence of the solution of the problem to the periodic functions $U^*(t)$ and $V^*(t)$, which is clearly observed in the following subsections.*

We divide the section into two different cases, depending on the choice of function h. For each case, we provide two examples where we consider two different functions $f(\mathbf{x}, t)$:

1. Firstly, we take
$$f(\mathbf{x}, t) = \frac{\cos t}{4 + \sin t} + \frac{x - y}{1 + t^2}, \tag{32}$$
in $(x, y) \in \Omega = [0, 1] \times [0, 1]$. Therefore, we can find the $2\pi-$periodic function
$$f^*(t) = \frac{\cos t}{4 + \sin t},$$
and then the asymptotic limit is
$$U^*(t) = \frac{4 + \sin(t)}{4 - \frac{\cos(t)}{2} + \frac{\sin(t)}{2}}.$$

2. Secondly, we consider
$$f(\mathbf{x}, t) = f^*(t) = \frac{2\cos(2t)}{2 + \sin(2t)} + \frac{\sin^2(t) + 2\sin(2t)}{1 + \cos^2(t)} \tag{33}$$
in $(x, y) \in \Omega = [0, 1] \times [0, 1]$. Hence, this time the $\pi-$periodic non-constant steady state is
$$U^*(t) = \frac{2 + \sin(2t)}{1 + \cos^2(2t)}.$$

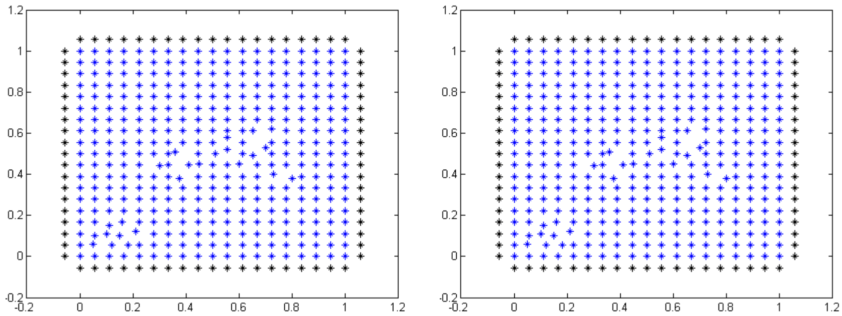

Fig. 1 Irregular clouds of points

3.1 Case 1

In this first case, we choose function $h(U, V)$ to be
$$h(U, V) = Ue^{-\chi V} - V, \tag{34}$$
which fulfils all assumptions made in [16], i.e., (3)–(6).

T(s)	3.72	6.86	13.14	16.28
$\|U - U^*(t)\|_{l^\infty(\Omega)}$	0.0436	0.0014	5.5900e-04	1.5783e-04
$\|V - V^*(t)\|_{l^\infty(\Omega)}$	0.1023	0.0088	3.9862e-04	2.1900e-04

Table 1 Values of $\|U - U^*(t)\|_{l^\infty(\Omega)}$ and $\|V - V^*(t)\|_{l^\infty(\Omega)}$ in the Example 1 and Case 1

3.1.1 Example 1

We select the following initial data

$$U_0(x, y) = e^{-10[(x-0.1)^2+(y-0.1)^2]} + e^{-10[(x-0.9)^2+(y-0.9)^2]},$$

$$V_0(x, y) = 0.7e^{-10[(x-0.5)^2+(y-0.5)^2]},$$

and parameters $\mu = 1, \chi = 0.3$. Table 1 shows the $\| \cdot |_{l^\infty}$ norm of the difference between the numerical solution and the asymptotic values U^*, V^* at several times. In Figure 2 and 3 we sketch the graphs of the periodic functions $U^*(t), V^*(t)$ (solid lines) and the most distant values of the discrete solution (that is to say, the value of the approximate solution where the greatest error in l^∞ norm is performed) at different times. As expected, the numerical

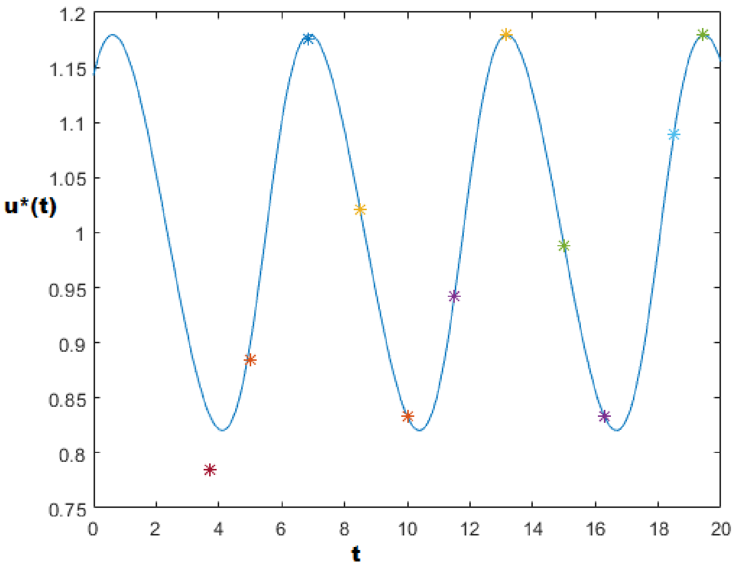

Fig. 2 The solid line corresponds to the graphic of the function $U^*(t)$, the stars to the value of the approximate solution u where we obtain the greatest error at 3.72, 5, 6.86, 8.5, 10, 11.5, 13.14, 15, 16.28, 18.5 and 19.42 in Example 1 and Case 1.

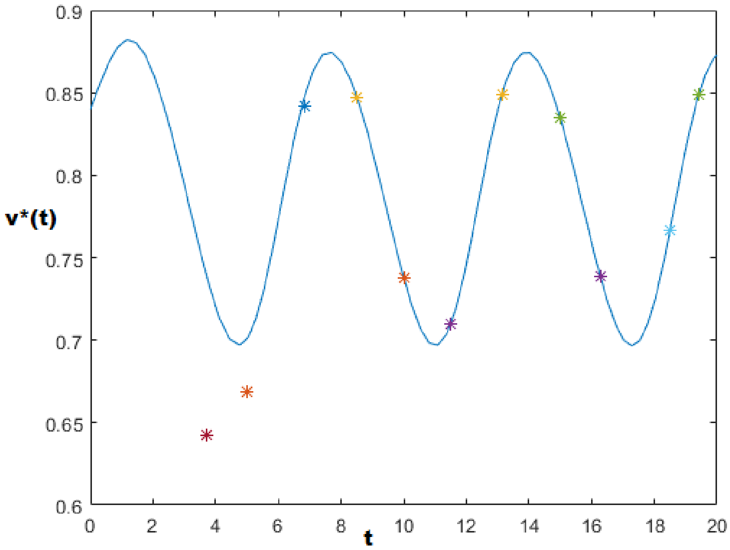

Fig. 3 The solid line corresponds to the graphic of the function $V^*(t)$, the stars to the most distant value of the approximate solution v at 3.72, 5, 6.86, 8.5, 10, 11.5, 13.14, 15, 16.28, 18.5 and 19.42 in Example 1 and Case 1.

results shown in Tables 1 and Figures 2 and 3, respectively, confirm the theoretical result of this paper (and also the ones in [16]). The numerical solution given by GFD scheme converges to the periodic asymptotic limit of system (1). In accordance with the theory, the approximate solution inherits the periodic behavior of the function f^* at large times.

T(s)	3.72	13.14	19.42
$\|U - U^*(t)\|_{l^\infty(\Omega)}$	0.0339	3.4624e-04	3.4304e-04
$\|V - V^*(t)\|_{l^\infty(\Omega)}$	0.0634	9.0783e-04	3.9845e-04

Table 2 Values of $\|U - U^*(t)\|_{l^\infty(\Omega)}$ and $\|V - V^*(t)\|_{l^\infty(\Omega)}$ in the Example 2 and Case 1

3.1.2 Example 2

We consider now the function given by (33) and initial data

$$U_0(x,y) = e^{-10[(x-0.2)^2+(y-0.2)^2]}, \quad V_0(x,y) = e^{-10[(x-0.8)^2+(y-0.8)^2]}$$

together with the parameters $\mu = 1, \chi = 0.3$.
As before, we illustrate in Table 2 the maximum difference between the limit value and the numerical solutions. Figure 4 and 5 reflect the periodic functions $U^*(t), V^*(t)$ (solid lines) and the values of the discrete solution at the node where the greatest error is achieved (stars) at different times.

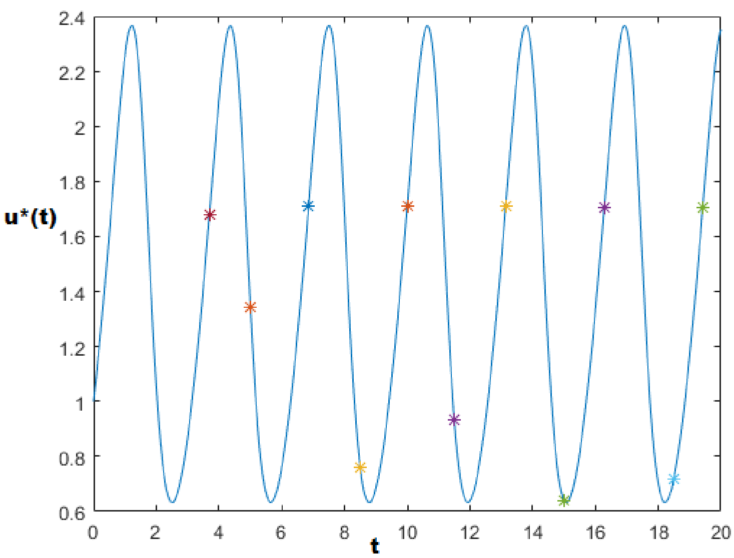

Fig. 4 The solid line corresponds to the graphic of the function $U^*(t)$, the stars to the value of the approximate solution, u, with the greatest error at times 3.72, 5, 6.86, 8.5, 10, 11.5, 13.14, 15, 16.28, 18.5 and 19.42 in Example 2 and Case 1.

As stated before, the convergence of the GFD scheme is clearly seen in the above figures. The numerical solution given by the explicit scheme behaves as the periodic functions (U^*, V^*) at t increases.

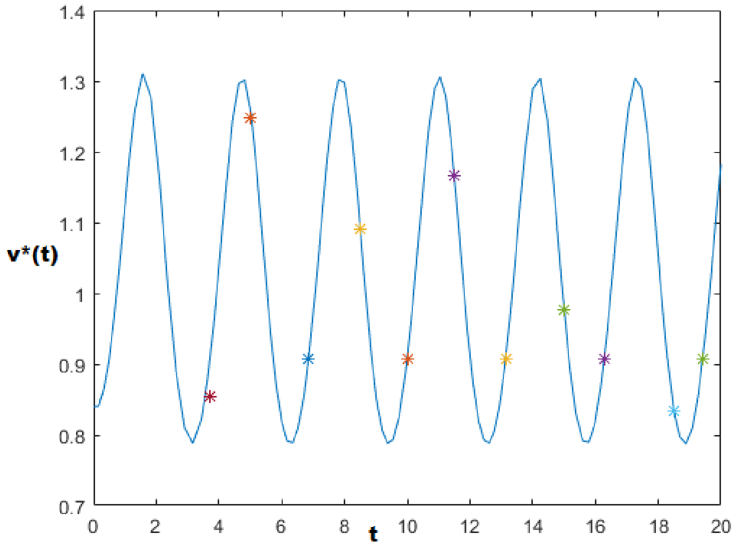

Fig. 5 The solid line corresponds to the graphic of the function $V^*(t)$, the stars to the value of the approximate solution, v, with the greatest error at times 3.72, 5, 6.86, 8.5, 10, 11.5, 13.14, 15, 16.28, 18.5 and 19.42 in Example 2 and Case 1.

3.2 Case 2

We consider now the function to describe the growth rate of the chemical substance

$$h(U,V) = \frac{Ue^{-\chi V} + V}{1+V} - V. \tag{35}$$

It is easily checked that h fulfils assumptions(3)–(6) (see also [16]). We provide two more examples with different functions $f(\mathbf{x}, t)$.

3.2.1 Example 3

Assume now that the initial data of this example are of the form

$$U_0(x,y) = 2e^{-10[(x-0.5)^2+(y-0.5)^2]}, \quad V_0(x,y) = e^{(x-0.5)^2+(y-0.5)^2},$$

and choose the parameters as $\mu = 1, \chi = 0.5$.

As previously mentioned, Table 3 shows the l^∞ norm of the difference between the solution given by the GFD scheme and asymptotic solution. Figure 6 and 7 present the behavior of the periodic functions $U^*(t), V^*(t)$ (solid lines) and the most distant values of the discrete solution at different times.

T(s)	3.72	6.86	10	16.28
$\|U - U^*(t)\|_{l^\infty(\Omega)}$	0.0093	0.0010	5.4652e-04	1.6059e-04
$\|V - V^*(t)\|_{l^\infty(\Omega)}$	0.0357	0.0026	4.1827e-04	6.6184e-05

Table 3 Values of $\|U - U^*(t)\|_{l^\infty(\Omega)}$ and $\|V - V^*(t)\|_{l^\infty(\Omega)}$ in the Example 3 and Case 2

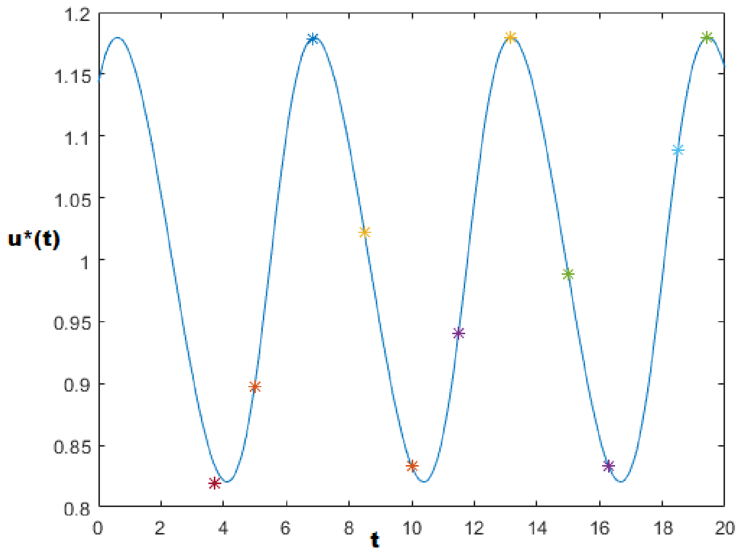

Fig. 6 The solid line corresponds to the graphic of the function $U^*(t)$, the stars to the value of the approximate solution, u, performing the greatest error at times 3.72, 5, 6.86, 8.5, 10, 11.5, 13.14, 15, 16.28, 18.5 and 19.42 in Example 3 and Case 2.

Tables 3 and Figure 6 and 7 show that, for any initial data, the discrete solution of (1) presents the same asymptotic periodic behavior of the continuous model, proved in [16]. For small times, the numerical solution may differ from the functions (U^*, V^*) since these represent the limit of the continuous solution and not the solution itself.

3.2.2 Example 4

Now we consider again

$$U_0(x,y) = e^{-10[(x-0.2)^2+(y-0.2)^2]}, \quad V_0(x,y) = e^{-10[(x-0.8)^2+(y-0.8)^2]},$$

and $\mu = 1, \chi = 0.5$ over the second cloud of points of Figure 1. In Table 4 we resume the maximum difference between the theoretical values U^*, V^* and the numerical solution. Figure 8 and 9 show the asymptotic limits of the problem (solid lines) and the values of the numerical solution (stars).

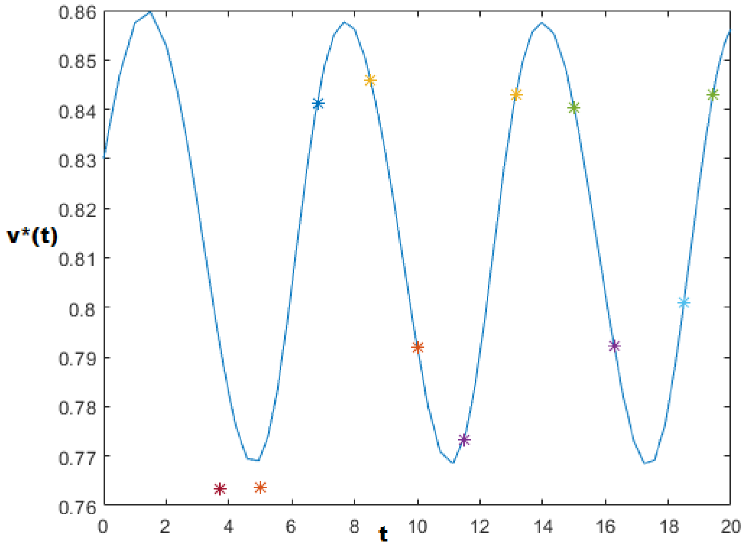

Fig. 7 The solid line corresponds to the graphic of the function $V^*(t)$, the stars to the value of the approximate solution, v, where we obtain the greatest error at times 3.72, 5, 6.86, 8.5, 10, 11.5, 13.14, 15, 16.28, 18.5 and 19.42 in Example 3 and Case 2.

T(s)	3.72	10	19.42
$\|U - U^*(t)\|_{l^\infty(\Omega)}$	0.0326	3.4328e-04	3.4302e-04
$\|V - V^*(t)\|_{l^\infty(\Omega)}$	0.0464	1.9974e-04	7.0348e-05

Table 4 Values of $\|U - U^*(t)\|_{l^\infty(\Omega)}$ and $\|V - V^*(t)\|_{l^\infty(\Omega)}$ in the Example 4 and Case 2

4 Conclusions

We have derived the discretization of the modified Keller-Segel system (1) by means of the GFD explicit scheme (19). Also, we have proved the conditional convergence of this scheme to the continuous model of the system and we have given the explicit conditions that the time increment, Δt must fulfil in order to obtain convergence of the method. An interesting remark from this proof is the fact that the condition for convergence relies strongly in the assumption of the continuous model, $\partial_V h < 0$. In order to illustrate the convergence of the Generalized Finite Difference Method for solving this PDE-ODE problem, and also the validity of the results stated in [16], we have provided four examples with different functions f and h, in the conditions [16], and tested the GFD method over two irregular cloud of points. As stated for the continuous model, and expected once we have proved the conditional convergence of the scheme, the discrete numerical solution converges to the asymptotic periodic functions

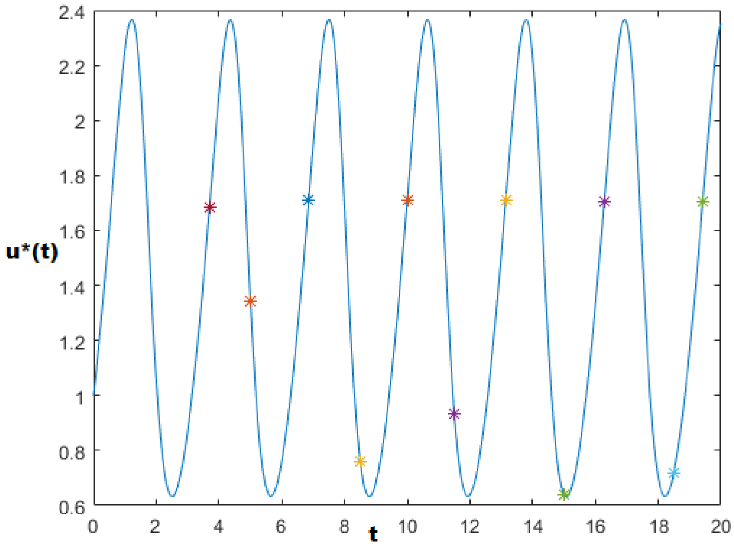

Fig. 8 The solid line corresponds to the graphic of the function $U^*(t)$, the stars to the value of the approximate solution, u, with the greatest error at times 3.72, 5, 6.86, 8.5, 10, 11.5, 13.14, 15, 16.28, 18.5 and 19.42 in Example 4 and Case 2.

$U^*(t), V^*(t)$. This means that some environmental periodicity conditions affect the behavior of the populations' density of a biological species, "U" and a chemical substance, "V", related by a chemotactic process.

The Generalized Finite Difference Method solves this strongly coupled highly nonlinear parabolic-ODE system efficiently and with high accuracy over regular and irregular domains. This means that this meshless method is an efficient tool for obtaining the numerical solution of this chemotaxis system appearing in Biology and Medicine.

Compliance with Ethical Standards:

Funding: the authors acknowledge the support of the Escuela Técnica Superior de Ingenieros Industriales (UNED) of Spain, project 2020-IFC02, and of the Universidad Politécnica de Madrid (UPM) (Research groups 2020). This work is also partially support by the Project MTM2017-83391-P DGICT, Spain.

Conflict of Interest: the authors declare that they have no conflict of interest.

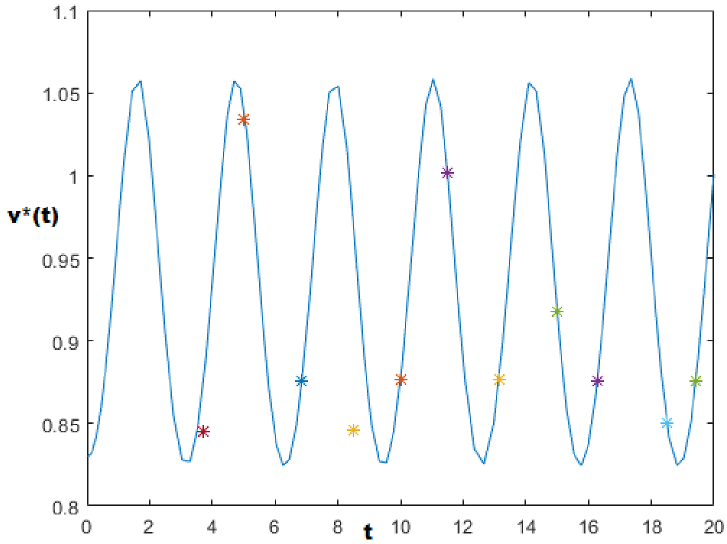

Fig. 9 The solid line corresponds to the graphic of the function $V^*(t)$, the stars to the value of the approximate solution, u, performing the greatest error at times 3.72, 5, 6.86, 8.5, 10, 11.5, 13.14, 15, 16.28, 18.5 and 19.42 in Example 4 and Case 2.

References

1. A.R. Anderson, M.A. Chaplain, *Continuous and discrete mathematical models of tumor-induced angiogenesis.* Bull Math Biol., **60** (5), 857–899, (1998).
2. Benito J. J., Ureña F., Gavete L. *Influence of several factors in the generalized finite difference method.* Applied Mathematical Modeling, **25**, 1039–1053, (2001).
3. Benito J. J., Ureña F., Gavete L. *Solving parabolic and hyperbolic equations by the generalized finite difference method.* Journal of Computational and Applied Mathematics, **209**, 208–233, (2007).
4. Benito J. J., García A., Gavete L., Negreanu M., Ureña F., Vargas A. M. *On the numerical solution to a parabolic-elliptic system with chemotactic and periodic terms using Generalized Finite Differences.* Engineering Analysis with Boundary Elements, **113**, 181-190, DOI: 10.1016/j.enganabound.2020.01.002, (2020)
5. Dehghan M., Abbaszadeh M., Mohebbi A., *A meshless technique based on the local radial basis functions collocation method for solving parabolic-parabolic Patlak-Keller-Segel chemotaxis model.* Engineering Analysis with Boundary Elements, **56**, 129–144, (2015).
6. Dunn GA., Zicha D. *Long-term chemotaxis of neutrophils in stable gradients: preliminary evidence of periodic behavior.* Blood Cells., **19**, 25–41, (1993).
7. Jensen, P.S., *Finite difference techniques for variable grids.* Comput. Struct., **2**, 17–29 (1972).
8. Keller EF., Segel LA. *Initiation of slime mold aggregation viewed as an instability.* J. Theoret. Biol., **26**, 399-415, (1970).
9. Keller EF., Segel LA. *A model for chemotaxis.* J. Theoret. Biol., **30**, 225-234, (1971).
10. Liszka T., Orkisz J., *The finite difference method at arbitrary irregular grids and its application in applied mechanics*, Comput. Struct., **11**, 83–95, (1980).
11. MacDonald G., Mackenzie J.A., Nolan M. Insall R.H., *A computational method for the coupled solution of reaction–diffusion equations on evolving domains and manifolds:*

Application to a model of cell migration and chemotaxis. J. Comput. Phys., **309**, 450–476, (2016).

12. Negreanu M., Tello J.I.,*Asymptotic stability of a two species chemotaxis system with non-diffusive chemoattractant.* J. Differential Equations, **258**, 1592–1617, (2015).
13. Negreanu M., Tello J.I., *On a Parabolic-ODE system of chemotaxis*, Discrete and Continuous Dynamical Systems - Serie S, **13** (2), 279–292, (2020).
14. Negreanu M., Tello J.I., Vargas A.M., *On a Parabolic-Elliptic chemotaxis system with periodic asymptotic behavior.* Math Meth Appl Sci., **42** (4), 1210-1226, (2019).
15. Negreanu M., Tello J.I., Vargas A.M., *On a fully parabolic chemotaxis system with source term and periodic asymptotic behavior.* Z. Angew. Math. Phys. (2020) 71:65, https://doi.org/10.1007/s00033-020-1282-0.
16. Negreanu M., Tello J.I., Vargas A.M., *A note on a periodic Parabolic-ODE chemotaxis system.*, Applied Mathematics Letters, https://doi.org/10.1016/j.aml.2020.106351.
17. Othmer H.G., A. Stevens A., *Aggregation, blowup, and collapse: The ABCs of taxis in reinforced random walks,* SIAM J. Appl. Math., **57**, 1044–1081, (1997).
18. Steinbock O., Hashimoto H., Müller SC. *Quantitative analysis of periodic chemotaxis in aggregation patterns of Dictyostelium discoideum.* Physica D: Nonlinear Phenomena, **49**, 233-239, (1991).
19. Ureña F., Benito J. J., Gavete L. *Application of the generalized finite difference method to solve the advection-diffusion equation.* Journal of Computational and Applied Mathematics, **235**, 1849–1855, (2011).
20. Ureña F., Gavete L., Garcia A., Benito J. J., Vargas A. M. *Solving second order nonlinear parabolic PDEs using generalized finite difference method (GFDM).* Journal of Computational and Applied Mathematics, **354**, 221-241, (2019).
21. Zusman, D.R., Scott, A.E., Yang, Z., Kirby, J.R. , *Chemosensory pathways, motility and development in Myxococcus xanthus.* Nat. Rev. Microbiol., **5** (11), 862–872, (2007).